THE DYNAMIC CHARACTERISTICS OF BRIDGE PIERS AS DESIGNED BY FOUR MAJOR SEISMIC DESIGN CODES

（Translation from Proceedings of JSCE, No.704/V-55, May 2002）



Hiromasa KIMATA　　Kongkeo PHAMAVANH　　Tada-aki TANABE

In order to clarify the features of various seismic design codes, nonlinear dynamic analysis of RC piers designed using standard seismic design codes of Japan, the United States, Europe, and New Zealand is carried out. The Lattice Equivalent Continuum Model (LECM) is adopted as the analytical method. A comparison of the analytical results clarifies the features of these various seismic design codes, and LECM is shown to be suitable for application to solving the dynamic problem.

Key Words: *seismic design code, seismic coefficient, response acceleration, ductility factor, lattice equivalent continuum model (LECM)*

Hiromasa KIMATA is an assistant professor in the Department of Civil Engineering and Environmental Design at Daido Institute of Technology, Japan. He obtained M. Eng. from the Nagoya University in 1995. His interest includes durability of concrete structures. He is a member of JSCE.

Kongkeo PHAMAVANH is a doctoral student in the Department of Civil Engineering at Nagoya University, Japan. He obtained M. Eng. from the Nagoya University in 2000. His interest includes nonlinear analysis of reinforced concrete structures. He is a member of JSCE.

Tada-aki TANABE is a professor in the Department of Civil Engineering at Nagoya University, Japan. He obtained D. Eng. from the University of Tokyo at 1971. He specializes in thermal crack of early age concrete and non-linear analysis of reinforced concrete structures. He is a fellow member of JSCE.

---

1. Introduction

The Hyogoken-Nambu Earthquake, which struck the Japanese city of Kobe on January 17, 1995, caused severe damage to a large number of civil structures, demanding substantial review of Japan's design codes for major structures including roads and railways. Since damage to reinforced concrete structures was particularly serious, the Japan Society of Civil Engineers (JSCE) promptly revised the Standard Specification for Design and Construction of Reinforced Concrete Structures. The sections related to seismic design, which had until then formed part of the "Construction" volume of the standards, were rearranged into a separate volume specifically for seismic design in July 1996, about a year and a half after the earthquake.
The damage caused by this great earthquake included devastation of reinforced concrete structures such as the pilz bridge of Hanshin Expressway and the ramen bridge of Sanyo Shinkansen (Bullet Train) Line. This was primarily because the design code applied to these structures in the 1960s assumed a maximum design earthquake motion of 0.2 G rather than the forces caused by an inland near-field earthquake such as the 1995 Hyogoken-Nambu event. Another critical factor was inferior knowledge at the time of construction of the properties of reinforced concrete members, resulting in overestimation of the allowable unit shear stress — a consequence of overestimating concrete shear capacity and lack of consideration of member ductility. Since then, design codes have been come up for revision one after another as various phenomena have been elucidated. Meanwhile, techniques for the numerical analysis of reinforced concrete structures have steadily progressed, contributing to further elucidation of their behavior.
Against the background of growing interest in comparing seismic design codes for reinforced concrete structures, design codes from four areas of the world were discussed at an international seminar held in Tokyo in April 1999 entitled "Comparative Performance of Seismic Design Codes for Concrete Structures." Researchers and structure designers representing the four codes reported on them [1], and trial design of bridge piers was then conducted by JSCE members using these codes. This was followed by an attempt to assess the characteristics of the codes by numerical analysis. However, the setting of certain design conditions was left to the discretion of each group of designers to allow for the characteristics of each code. This resulted in differences between the conditions under which each code was tested, such as different pier cross-sectional dimensions. As a result of this, distinctions between the codes could not be clarified by comparison of the numerical analysis results [2], [3]. In this study, the trial design of bridge piers is once again carried out, in this case with identical cross-sectional dimensions of the piers, with the aim of elucidating the characteristics of each code. The dynamic properties of the piers were examined by nonlinear numerical analysis.
The accuracy of techniques for the numerical analysis of concrete structures has improved as progress has been made in the modeling of the constitutive laws of concrete, which is a heterogeneous material. Highly accurate analysis is now available using models derived from precise theoretical considerations. However, numerical analysis techniques have yet to be established for static behavior of concrete under repeated loading and for dynamic behavior in the true sense of the word, since the mechanical properties of concrete under alternating loading as well as opening/closing behavior and boundary stress transfer at cracking have not been fully elucidated. A clarification of these phenomena is crucial to establishment of more accurate dynamic analysis techniques useful in verifying the dynamic performance of structures, streamlining the design procedure, and determining residual deformation and available performance immediately after an earthquake (which affect post-earthquake repair and retrofitting).
The lattice equivalent continuum model (LECM) is a modeling method for reinforced concrete members in which cracked concrete and reinforcement are replaced by lattices so as to derive an equivalent continuum constitutive equation. LECM has been proven capable of accurately expressing the static behavior of reinforced concrete members even under repeated loading [4], [5]. This model is used as an analysis technique in this study.

2. Four seismic design codes

(1) Overview
This study involved the trial design of bridge piers using seismic design codes from four parts of the world: Japan's Standard Specification for Design and Construction of Concrete Structures published by the Japan Society of Civil Engineers (JSCE), the USA's California Department of Transportation Standard (Caltrans), the EC's Eurocode 8 (EC8), and New Zealand's Standards New Zealand (NZs). Editions of these standards current in April 1999, as introduced in the above-mentioned seminar, were used in the study.
The seismic design of a structure basically follows the procedure shown in Fig. 1 in all cases. The various codes are distinguished by their handling of "calculation of design horizontal force" and "verification of

required reinforcement ratio" among other parts of the procedure. Safety factors for material strengths and load-carrying capacity also vary from one code to another. The main characteristics of the four codes are summarized in the following sections.

(2) JSCE (Japan)

The design procedure set out in the JSCE code is shown in Fig. A1 in the Appendix [1],[6],[7]. Earthquake motion is classified into two levels: Level 1 (earthquake motion of a magnitude encountered a few times during the expected working life of a structure) and Level 2 (strong earthquake motion of a magnitude rarely encountered during the working life of a structure). A structure is designed so that it meets Seismic Performance Requirement 1 under Level 1 earthquake motion (meaning that there is sufficient safety against compressive failure of the concrete during an earthquake with no reinforcement yielding) and Seismic Performance Requirement 2 (meaning the response displacement and residual displacement are within allowable limits in the case of an earthquake) or Seismic Performance Requirement 3 (meaning the frame of the structure is left intact) under Level 2 earthquake motion.

Figure 2 compares the response spectra used for the four codes. The fine lines in the figure represent the spectra under Level 1G (seismic waves causing a maximum acceleration of approximately 400 gal and an elastic response spectrum peak of approximately 1 G). The bold lines represent the spectra under Level 2G (seismic waves causing a maximum acceleration of approximately 800 gal and an elastic response spectrum peak of approximately 2 G). These correspond to response spectra under Case A and Case B earthquake motions as described later in this paper.

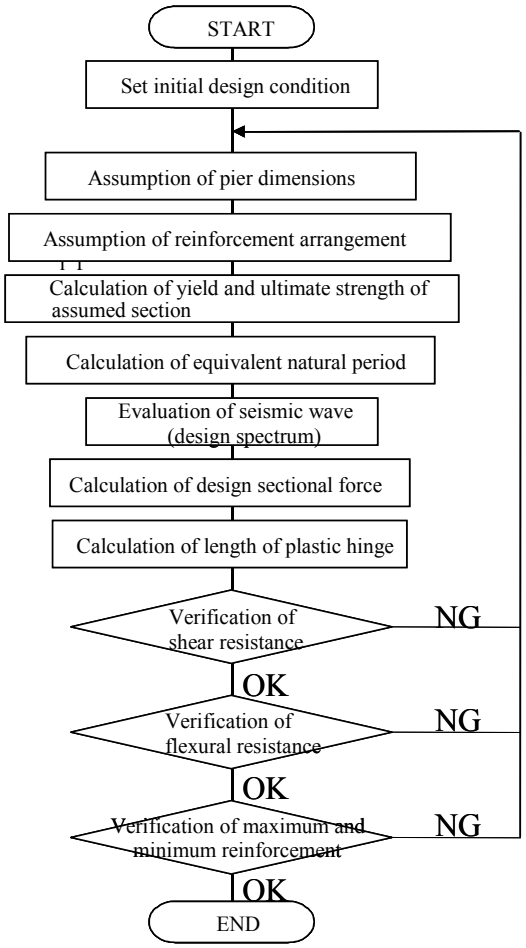

Figure 1 Flowchart of general seismic design

Though the levels of earthquake motion to be considered at the design stage is given in the text, no specific spectra are laid down in the JSCE code. The response spectra shown in Fig. 2(a) were therefore adopted as the spectra by JSCE. These are elastic response spectra under Type I and Type II earthquake motions (Type I ground) used in the ultimate horizontal strength method during an earthquake specified in the Standard Specification for Road Bridges, Volume V: Seismic Design [8].

According to the JSCE code, the design horizontal seismic coefficient K_h is determined using the following equation based on the equal energy rule:

$$K_h = \frac{K_{h0}}{\sqrt{2\mu_d - 1}} \tag{1}$$

where K_{h0} = elastic response spectrum

μ_d = design ductility factor

Though the JSCE code does not consider the effect of biaxial bending, it confirms safety by separate verifications in the direction of bridge axis and bridge width.

The specified range of longitudinal reinforcement ratio is between a maximum of 6.0% and a minimum of 0.15%, which is the widest range among the four codes. The transverse bar spacing is specified as not more than the smallest of the following: 12 times the diameter of the longitudinal bars, half the cross-sectional depth, or 48 times the transverse bar diameter. This is much greater than specified by the other codes. A more stringent requirement is considered necessary from the viewpoint of preventing buckling of longitudinal bars.

The JSCE code is characterized by the requirement for verification of response displacement of members (ductility factor), which is not found in the other codes.

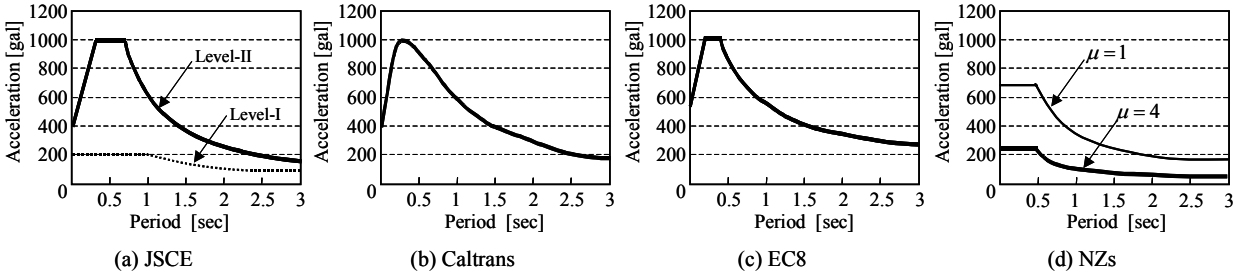

Figure 2 Design seismic coefficients for level 1G and 2G earthquake loading

(3) Caltrans (U.S.A.)

The design procedure specified by Caltrans is shown in Fig. A2 in the Appendix [1]. Caltrans uses the elastic response spectra shown in Fig. 2 (b). Instead of using the equal energy rule, the design horizontal seismic coefficient is determined using a reduction coefficient, Z, as follows:

$$K_h = \frac{K_{h0}}{Z} \tag{2}$$

This reduction coefficient of response spectra, Z, is obtained from the ratio of the natural period, T^*, determined from the ground properties to the equivalent natural period, T, of the member. The specified maximum value of Z is 3.0, which corresponds to μ_d = 5.0 if the concept of the equal energy rule is applied.

Caltrans incorporates the effect of biaxial bending of piers by multiplying the design sectional force by 1.4. Also, the verification of reinforcement content is more stringent than that of the JSCE code. For transverse reinforcing bars in particular, the reinforcement content is verified separately for the plastic hinge zone, a general zone, and the end zone. Transverse bar spacing is required to be not more than the smallest of the following: 6 times the longitudinal bar diameter, 0.2 times the depth or width of the pier cross-section, or 20cm. This is less than half the value required by the JSCE code. The ratio of longitudinal reinforcement is required to be within the range of 4.0% and 1.0%, the narrowest of the four codes.

(4) Eurocode 8 (Europe)

The design procedure specified by EC8 is shown in Fig. A3 in the Appendix [1]. The EC8 code uses elastic response spectra as shown in Fig. 2(c). EC8 does not use the equal energy rule, either. instead, the design horizontal seismic coefficient is determined using a coefficient, q, that is similar to coefficient Z in Caltrans:

$$K_h = \frac{K_{h0}}{q} \tag{3}$$

The maximum value of q is specified as 3.5, which corresponds to μ_d = 6.67 in the equal energy rule concept.

EC8 incorporates the effect of biaxial bending by multiplying the acceleration of earthquake motion by 1.3. EC8 is also characterized by more conservative design requirements, such as underestimation of the yield moment and ultimate moment and neglecting of the contribution of concrete to member shear capacity under certain conditions.

Though no amount of longitudinal reinforcement is specified, verification of the minimum transverse reinforcement content is strictly required from the standpoint of preventing buckling of longitudinal bars.

(5) NZs (New Zealand)

The design procedure specified by NZs is shown in Fig. A4 in the Appendix [1]. In contrast to the other codes, NZs adopts non-elastic response spectra, as shown in Fig. 2(d). Response spectra are therefore selected according to the design ductility factor of the member.

The design horizontal seismic coefficient is determined by multiplying the response spectra by zone coefficient Z, risk coefficient R, and structure coefficient S_p.

$$K_h = Z \cdot R \cdot S_p \cdot K_{h0} \tag{4}$$

NZs takes into detailed account the influence of the P-Δ effect in calculating the design section force. Moreover, in consideration of the simultaneous vertical acceleration that may occur during an earthquake, the axial force is multiplied by 1.3 and 0.8 in the downward and upward directions, respectively, assuming respective accelerations of 0.3 G and 0.2 G in these directions. Verification is carried out under more stringent conditions.
The effect of biaxial bending is incorporated by multiplying the design moment by 1.04. The longitudinal reinforcement ratio is required to be between 5.2% and 0.8%. The transverse bar spacing is required to be no more than 6 times the longitudinal bar diameter and not more than 1/4 the depth of the pier cross-section, which is almost equivalent to the requirements of Caltrans and EC8. In addition, a minimum transverse reinforcement content is specified.

3. Trial design of reinforced concrete piers

(1) Overview
Two types of piers were designed in accordance with the four seismic design codes, using the same input ground motion, ground type, superstructure weight, materials, and pier shape. The shape and dimensions of the pier cross-section were also equalized so as to prevent wide variations in pier rigidity, thereby facilitating the comparison of analysis results.

(2) Design conditions
(a) Earthquake load
There are regional differences in the characteristics of historical earthquake motion, so the specifications made in each code vary. This makes it very difficult to set up common earthquake load conditions. Two types of earthquake motion, leading to maximum response accelerations of 1 G and 2 G as shown in Fig. 3, were selected for this study. These waveforms, which result in maximum accelerations of 400 and 800 gal, are referred to as Cases A and B, respectively. They correspond to Type I and Type II seismic waveforms as specified in the Japanese Standard Specification for Road Bridges [8].
The Case B waveform is the N-S component of the record taken at Kobe Maritime Observatory during the Hyogoken-Nambu Earthquake.
(b) Form of structure
The structure under analysis is a single pier 7 m in height designed to support an elevated expressway as shown in Fig. 4. The square cross section of the pier measures 1.5 by 1.5 m in Case A and 2.0 by 2.0 m in Case B. The superstructure has a span of 40 m and a width of 10 m, and is assumed to impose a load of 7,000 kN corresponding to the dead load of an expressway typical of those constructed in Japan.
In this analysis, the live load is ignored, and only seismic action in the direction of the road axis is considered.
(c) Ground conditions
Since evaluating the compound behavior of structure and ground is very complicated, it is assumed that the pier is constructed on rigid bed-rock and that the earthquake motion acts directly on the base of the pier.
(d) Materials
The concrete used in the design is of compressive strength 24 N/mm^2. The reinforcing steel is JIS SD 345 with a yield strength of 345 N/mm^2. The common design conditions are tabulated in Table 1.
(e) Bar arrangement
For the reasons mentioned above, the shape and dimensions of the pier section are equalized. The characteristics of each code are therefore represented only by the bar arrangement. Longitudinal bars are arranged uniformly in the road axis and road width directions so as to impart equal load-carrying capacity and deformation performance in both directions.

(3) Specifications of designed pier
Table 2 gives the specifications of the eight piers designed according to the requirements of the four codes. The bar arrangements are shown in Figs. A5 to A8. In cases where the elastic response spectrum for the more intense seismic waves, corresponding to Case B, is not indicated in the code, the spectrum given in the code is simply multiplied by an appropriate factor.
The load-carrying performance and deformation performance of a pier vary widely depending on the ductility factor adopted in design. Whereas the JSCE and NZs codes require the design ductility factor to be determined, no such value is required in Caltrans and EC8. It is therefore difficult to deal with the design ductility factor at the condition setting stage of the procedure. As stated in the previous section, the spectrum reduction coefficient is set at between 1 and 3.5 depending on ground conditions. In the equal energy rule,

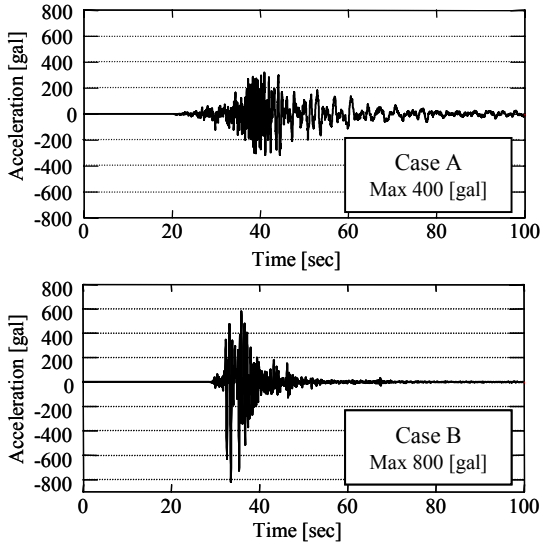

Figure 3 Two seismic waves forms

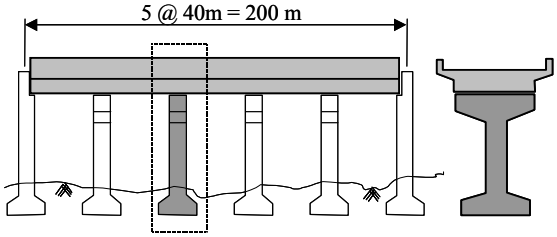

Figure 4 Outline of bridge pier for trial design

the spectrum reduction coefficient is determined by the design ductility factor, μ_d. A reduction coefficient between 1 and 3.5 corresponds to μ_d = 1 to 6.67 when converted by the equal energy rule. An intermediate value of 4 is therefore adopted as the design ductility factor for the trial design in accordance with the JSCE and NZs codes.

The longitudinal reinforcement ratio in Case B according to the Caltrans code is 6.48%, exceeding the specified maximum of 4.0%. Since reducing the ratio to the specified level would require an increase in pier cross section, a higher longitudinal reinforcement ratio was adopted so as to avoid excessive difference between the cross-sectional areas in Case A and Case B designs.

Table 1 Common design requirements

Structure	Reinforced concrete pier (square cross section, length= 7m and 30m)
Type of foundation	Direct foundation
Weight of superstructure	7000 [kN] (live loads not considered)
Design ground acceleration	400, 800 [gal]
Grade of concrete	24 [N/mm^2] (JIS)
Grade of steel	345 [N/mm^2] (SD345, JIS)

Table 2 Summary of Designed Pier Sections

	Case A (7m column, 400gal wave)			
	JSCE	Caltrans	Euro	NZ
Section [mm×mm]	1500×1500			
Main Bars	52-D51	96-D32	96-D29	40-D32
Ratio of Main Bars [%]	4.68	3.38	3.38	1.41
Tie Bar	4-D22	8-D16	8-D19	8-D13
Ratio of Tie Bars [%]	0.69	0.71	0.76	0.38
Natural Period [sec]	0.572	0.694	0.713	0.852
	Case B (7m column, 800gal wave)			
	JSCE	Caltrans	Euro	NZ
Section [mm×mm]	2000×2000			
Main Bar	60-D51	128-D51	112-D51	112-D41
Ratio of Main Bars [%]	3.04	6.48	5.67	3.75
Tie Bars	4-D25	8-D16	8-D22	10-D19
Ratio of Tie Bars [%]	1.01	1.47	1.03	0.71
Natural Period [sec]	0.376	0.223	0.330	0.375

4. Numerical analysis by LECM

(1) Overview

To make the complex structural problem easier to solve, an attempt is made to model the continuous structural member with lattice members as shown in Fig. 5. Structures are assumed to be collections of

lattices, and the behavior of the structure can be clarified by appropriately selecting the number, orientation, and rigidity of these lattices. Even if the structure to be analyzed is non-elastic, as in the case of reinforced concrete, highly accurate analysis is possible by adding nonlinearity to the stress-strain relation of the lattice.

The successful use of discrete lattice modeling of a reinforced concrete element by Niwa et.al. [9], [10] has led the authors to develop the lattice equivalent continuum model to allow for wider and more flexible application of the concept.

The lattice equivalent continuum model (LECM) is an analytical method of leading the constitutive equation of cracked RC elements by arranging the lattice in the direction of the principal stress. As shown in Fig. 6, lattices are used only to derive the continuum constitutive equation, and analysis is done by normal FEM. Unlike typical plastic theory, LECM is not complex in that the constitutive equation of the lattice may make use of the equivalent uni-axial stress-strain relationship.

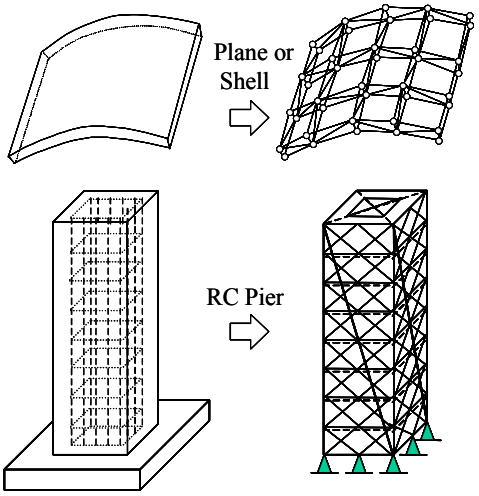

Figure 5 Examples of structures modeled with lattice

(2) Transformation of strain and stress-strain relationship

When the stress and strain caused in a continuous plane body are given by $\sigma = [\sigma_x \ \sigma_y \ \tau_{xy}]^T$ and $\varepsilon = [\varepsilon_x \ \varepsilon_y \ \gamma_{xy}]^T$ respectively, the stress and strain in the $\xi - \eta$ coordinate system at rotation angle ϕ to the $x - y$ coordinate system can be written as follows [12]:

$$\begin{Bmatrix} \varepsilon_\xi \\ \varepsilon_\eta \\ \gamma_{\xi\eta} \end{Bmatrix} = \begin{bmatrix} \cos^2\phi & \sin^2\phi & \sin\phi\cos\phi \\ \sin^2\phi & \cos^2\phi & -\sin\phi\cos\phi \\ -2\sin\phi\cos\phi & 2\sin\phi\cos\phi & \cos^2\phi - \sin^2\phi \end{bmatrix} \begin{Bmatrix} \varepsilon_x \\ \varepsilon_y \\ \gamma_{xy} \end{Bmatrix} \quad (5)$$

$$\begin{Bmatrix} \sigma_\xi \\ \sigma_\eta \\ \tau_{\xi\eta} \end{Bmatrix} = \begin{bmatrix} \cos^2\phi & \sin^2\phi & 2\sin\phi\cos\phi \\ \sin^2\phi & \cos^2\phi & -2\sin\phi\cos\phi \\ -\sin\phi\cos\phi & \sin\phi\cos\phi & \cos^2\phi - \sin^2\phi \end{bmatrix} \begin{Bmatrix} \sigma_x \\ \sigma_y \\ \tau_{xy} \end{Bmatrix} \quad (6)$$

In LECM, the first step is to replace each cracked RC member with a lattice. The lattices are arranged in the direction of principal strain in the concrete and the direction of the steel bars. If the uniaxial lattice strain is assumed to be $\{\hat{\varepsilon}\} = [\varepsilon_1 \cdots \varepsilon_i \cdots \varepsilon_n]^T$, the following expression is obtained:

$$\{\hat{\varepsilon}\} = \begin{bmatrix} \cos^2\alpha_1 & \sin^2\alpha_1 & \sin\alpha_1\cos\alpha_1 \\ \vdots & \vdots & \vdots \\ \cos^2\alpha_i & \sin^2\alpha_i & \sin\alpha_i\cos\alpha_i \\ \vdots & \vdots & \vdots \\ \cos^2\alpha_n & \sin^2\alpha_n & \sin\alpha_n\cos\alpha_n \end{bmatrix} \begin{Bmatrix} \varepsilon_x \\ \varepsilon_y \\ \gamma_{xy} \end{Bmatrix} = [L_\varepsilon]\{\varepsilon\} \quad (7)$$

where n is the number of lattices. Similarly, if the uniaxial stress of the lattice is assumed to be $\{\hat{\sigma}\} = [\sigma_1 \cdots \sigma_i \cdots \sigma_n]^T$, the following expressions are obtained:

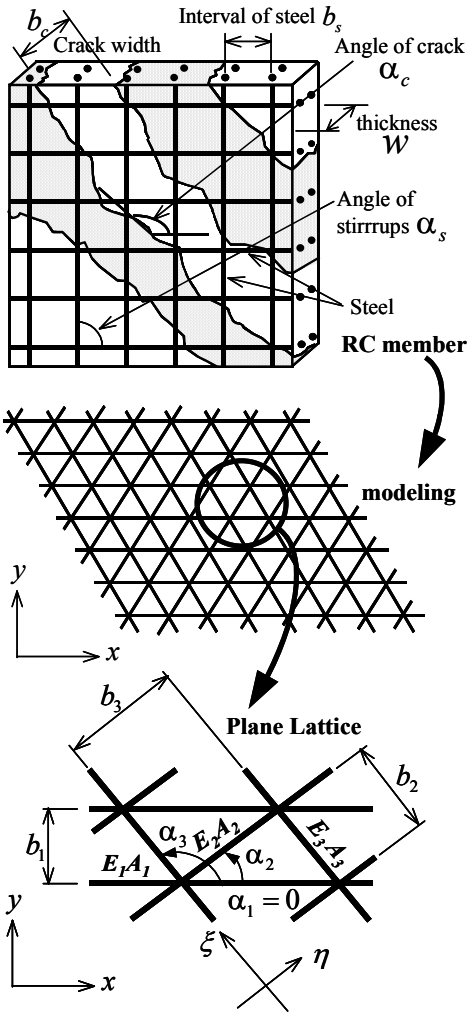

Figure 6 A continuation object plane and plane lattice

$$\{\hat{\sigma}\}=\begin{bmatrix} r_1 & & & & \\ & \ddots & & 0 & \\ & & r_i & & \\ & 0 & & \ddots & \\ & & & & r_n \end{bmatrix}\{\hat{\varepsilon}\}=[R]\{\hat{\varepsilon}\} \tag{8}$$

$$r_i=\frac{E_i A_i}{b_i} \tag{9}$$

where E_i, A_i, and b_i are the elastic modulus, sectional area, and positional interval of the lattices, respectively. Moreover, the stress $\{\sigma\}$ of a continuous body can be written as follows in terms of the stress $\{\hat{\sigma}\}$ of the lattices by using the stress rotation matrix:

$$\{\sigma\}=\begin{bmatrix} \cos^2\alpha_1 & \cdots & \cos^2\alpha_i & \cdots & \cos^2\alpha_n \\ \sin^2\alpha_1 & \cdots & \sin^2\alpha_i & \cdots & \sin^2\alpha_n \\ \sin\alpha_1\cos\alpha_1 & \cdots & \sin\alpha_i\cos\alpha_i & \cdots & \sin\alpha_n\cos\alpha_n \end{bmatrix}\{\hat{\sigma}\}=[L_\varepsilon]^T\{\hat{\sigma}\} \tag{10}$$

Then Eqs. (7) and (8) are substituted into Eq. (10):

$$\{\sigma\}=[L_\varepsilon]^T[R][L_\varepsilon]\{\varepsilon\}=[D]\{\varepsilon\} \tag{11}$$

And the stiffness matrix $[D]$ for the continua is obtained as follows:

$$[D]=\begin{bmatrix} \sum_{i=1}^{n} r_i\cos^4\alpha_i & \sum_{i=1}^{n} r_i\sin^2\alpha_i\cos^2\alpha_i & \sum_{i=1}^{n} r_i\sin\alpha_i\cos^3\alpha_i \\ & \sum_{i=1}^{n} r_i\sin^4\alpha_i & \sum_{i=1}^{n} r_i\sin^3\alpha_i\cos\alpha_i \\ \textit{sym.} & & \sum_{i=1}^{n} r_i\sin^2\alpha_i\cos^2\alpha_i \end{bmatrix} \tag{12}$$

Thus, by using plane lattices, the stiffness matrix of the continua can be introduced.

(3) Application to two-dimensional RC element

In applying the matrix represented by Eq. (12) to a 2D RC element, it is necessary to obtain r_i in the $[D]$ matrix. Here, r_i comprises elastic modulus, sectional area, and the positional interval of the lattices. The value of r_i for the steel bar can be obtained directly, but for the concrete it must be obtained in consideration of the influence of cracks. Given that the sectional area of a concrete part is the product of crack interval b_c and thickness w, r_i at the concrete can be written as follows:

$$r_i=\frac{E_c A_c}{b_c}=\frac{E_c b_c w}{b_c}=E_c w \tag{13}$$

where E_c is the elastic modulus of concrete and w is the thickness of a concrete element. Thus, r_i for the concrete does not depend on the crack interval.

Once a crack enters a concrete part , the rigidity of the RC material is replaced with a lattice and it leads, while both concrete and reinforced concrete are handled as elastic bodies prior to cracking.

Before the crack occurs in concrete, concrete and steel bar are handled as an elastic body, and after the crack occurs, the stiffness of RC element is introduced by lattices. The stiffness matrix of the concrete and steel before a crack enters the concrete element can be written as follows:

$$[D_c]=\frac{E_c}{1-\nu^2}\begin{bmatrix} 1 & \nu & 0 \\ \nu & 1 & 0 \\ 0 & 0 & \frac{1-\nu}{2} \end{bmatrix}, \qquad [D_s]=\begin{bmatrix} E_s & 0 & 0 \\ 0 & E_s & 0 \\ 0 & 0 & 0 \end{bmatrix} \tag{14}$$

where E_c and E_s are the initial elastic moduli of the concrete and steel, and ν is Poisson's ratio for concrete.
In this technique, the element thickness is included in the constitutive equation. If the concrete and steel thickness is assumed to be t_c and t_s respectively, the entire $[D]$ matrix is then,

$$[D] = t_c[D_c] + t_s[D_s]$$

The principal stress of each element is calculated, and a crack is assumed to occur when the principal stress exceeds the uniaxial tensile strength or 1/2 of the compression strength of the concrete. The direction of principal stress at this time is the orientation in which the lattice is arranged.
The stiffness matrix for cracked RC elements is introduced by following the above procedure. The crack angle in a particular element is different from that in adjoining elements.

(4) Stress-strain relationship of materials
The repeated uniaxial stress-strain relationships for the lattice used in this analysis are shown in Fig. 7. The element stiffness matrix for RC elements can be introduced very easily by using a simple equivalent uniaxial stress-strain relationship.

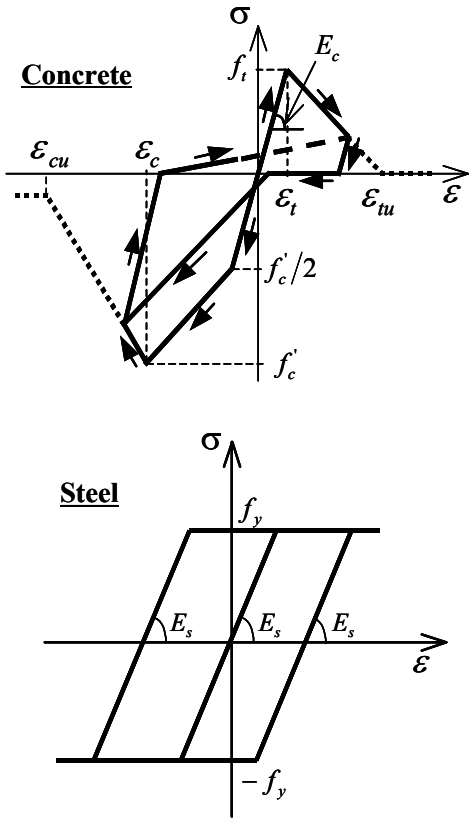

Figure 7 Equivalent uniaxial stress-strain relationship

5. Analysis results and discussion

(1) Outline of analysis
The analysis model the pier is shown in Fig. 8. In pushover analysis, monotonic loading was applied to the pier top under displacement control. In dynamic analysis, two different input seismic waveforms, as shown in Fig. 3, were applied directly to the pier base. It should be noted that the damping matrix of the equation of motion was assumed to be zero in the dynamic analysis to help distinguish the properties of the different piers. The Newmark β method [13] was used for numerical integration.

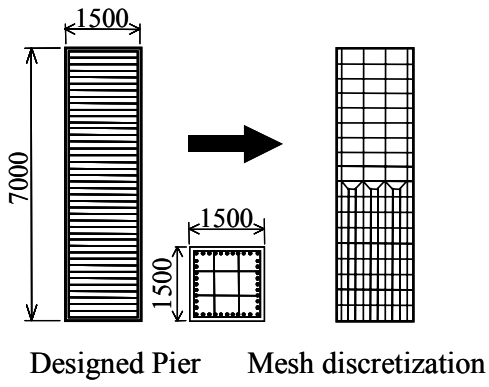

Figure 8 Shape of pier and analytical model (Case A)

(2) Pushover analysis
The results of pushover analysis are shown in Fig. 9. All piers failed in flexure.
In Case A, the JSCE code gave the greatest flexural capacity at 3,966 kN, while NZs gave the smallest at 1,323 kN. The added-moment effect can cause concern when displacement exceeds 125 mm, particularly in the case of the NZs piers with their low flexural capacity. However, the effect was judged marginal for the range of displacements studied in this analysis, since the numerical analysis incorporates geometric nonlinearity and the ratio of added moment to the horizontal loading moment is as low as 2% to 3% due to the high flexural capacity of all piers except NZs.
The analysis results for the Caltrans and EC8 piers are almost identical, despite slightly different transverse reinforcement ratios. This is because they have the same longitudinal reinforcement ratio. One of the reasons for the high flexural capacity of the JSCE piers is the greater response spectrum than piers designed by other codes near the resonance point. Figure 10 shows the response spectrum and equivalent natural period of piers made in accordance with each code. The largest difference among response spectra among the four codes is the range of the maximum values near the resonance point. The range is narrowest for Caltrans piers

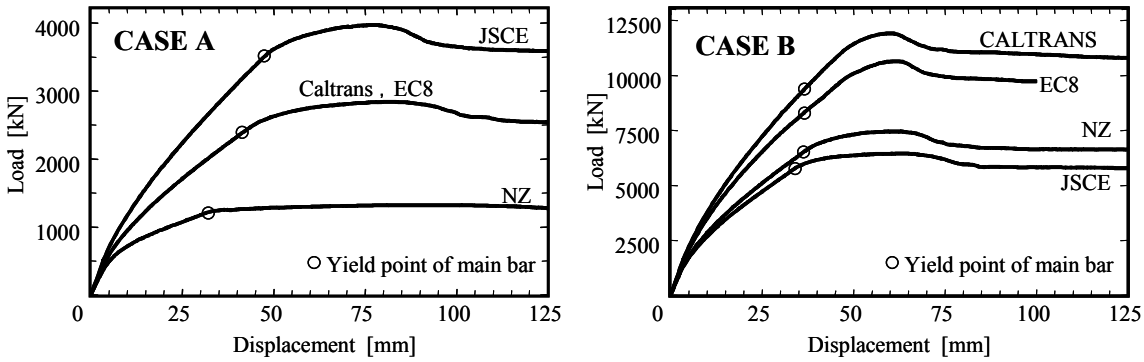

Figure 9 Analytical results (pushover)

and widest for JSCE piers. Though there is no appreciable difference in the natural frequencies of the four piers, the wide range of maximum values of the JSCE spectrum leads to a greater horizontal seismic coefficient than for piers designed by the other codes, resulting in greater flexural capacity. These response spectra characteristics are particularly distinct in Case A.

In Case B, Caltrans and EC8 led to higher flexural capacities than JSCE and NZs. Capacity was greatest with Caltrans at 12,152 kN and smallest with JSCE at 6,436 kN. The greater capacity of the Caltrans design results from the lowest reduction coefficient of the response spectra among the four, at 1.628, which in turn represents the greatest design horizontal seismic coefficient.

Table 3 gives the shear capacity ratio as obtained for each code; i.e., the ratio of shear capacity in the plastic hinge zone obtained from analysis to the value calculated using the equations specified in each code. The safety of a structure against shear failure increases as the shear capacity ratio increases. Differences among the equations for calculating the shear capacity are marginal, as the contribution of the transverse reinforcement is derived from the same truss theory [14], though the methods of calculating the contribution made by the concrete vary slightly. The shear capacity ratios of all piers exceeded unity, proving them safe against shear failure. The JSCE and NZs piers, which have low flexural capacity, are found to possess adequate margins against shear failure. The Caltrans pier also exhibits a good margin, but the EC8 pier shows a slightly lower value. This is because, in the EC8 code, the shear capacity of a member is calculated based only on the effect of the transverse reinforcement without considering the contribution of the concrete under shear forces when the ratio of the stress resulting from the dead load and superimposed load to the compressive strength, η_k, is under 0.1. However, since η_k exceeds 0.1 in both cases analyzed here, the concrete contribution was incorporated. This causes a reduction in the required transverse reinforcement, resulting in a slightly smaller margin against shear failure. However, the shear capacity of actual piers designed in accordance with EC8 is deemed sufficient, since the cross-sectional area would be designed such that η_k would be less than 0.1. With a larger cross section, a pier designed in accordance with EC8 can be expected to exhibit a shear capacity greater than that resulting from the other codes.

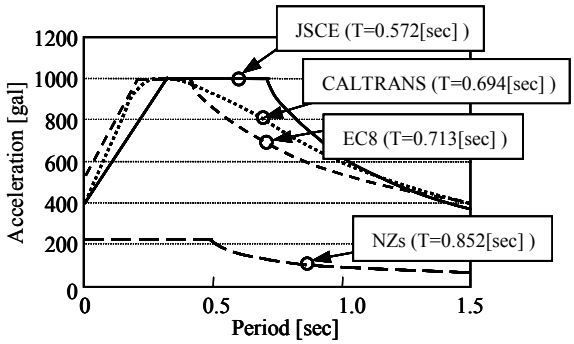

Figure 10 Comparison of elastic response spectra

Table 3 Shear capacity ratio

	Case A			
	JSCE	Caltrans	EC8	NZs
V_d [kN]	4923	4824	4018	4507
V_a [kN]	3966	2840	2839	1322
V_a/V_d	1.241	1.699	1.415	3.409
	Case B			
	JSCE	Caltrans	EC8	NZs
V_d [kN]	11564	23384	11691	10732
V_a [kN]	6436	12152	10633	7444
V_a/V_d	1.797	1.924	1.100	1.442

(3) Dynamic analysis

Figure 11 shows the results of dynamic analysis superimposed on the results of the pushover analysis. This is the relationship between pier top displacement and shear force. In all cases, the first mode predominates over other modes in pier deformation.

Similarly to the results of the pushover analysis, greater response displacement is exhibited by NZs in Case A and by the JSCE code in Case B.

Caltrans and EC8 led to small response displacements, particularly in Case B. This can be attributed to the fact that Caltrans and EC8 apply a more conservative design process than the JSCE code and NZs, such as by using a higher design horizontal seismic coefficient. This is because these codes do not include direct investigation of the deformability of members and must also take account of the effect of biaxial bending.

Figure 12 shows the response plasticity factor, or the value obtained by dividing the maximum response displacement in dynamic analysis by the yield displacement obtained in pushover analysis. Also shown in the figure is the design ductility factor. The values for Caltrans and EC8 are reduction coefficients Z and q converted by the equal energy rule for the purpose of comparison. Though the response plasticity factors of piers are higher in Case A than in Case B, most remain within the range of the design ductility factor.

The JSCE code requires verification of member ductility at the design stage. Whereas the effect of slip-out of longitudinal bars is incorporated in the calculation equation, it is not incorporated in the analysis. Nevertheless, the response plasticity factors of the two JSCE piers are close to the design ductility factor, and the differences is the smallest among the four codes. Despite arguments about the accuracy of the equal energy rule [15], its use is considered to have led to appropriate design seismic coefficients in the trial design of piers using the JSCE code in this case.

The response plasticity factor of the NZs pier in Case A exceeded the design ductility factor. Similar results have been reported by numerical analysis using a model different from that used in the present study [2], but this is not attributable to the numerical analysis technique. According to the numerical analysis of multiple piers in these cases of trial design, piers designed in accordance with NZs tend to permit slightly greater deformation than piers by other codes. This is particularly evident in the Case A pier.

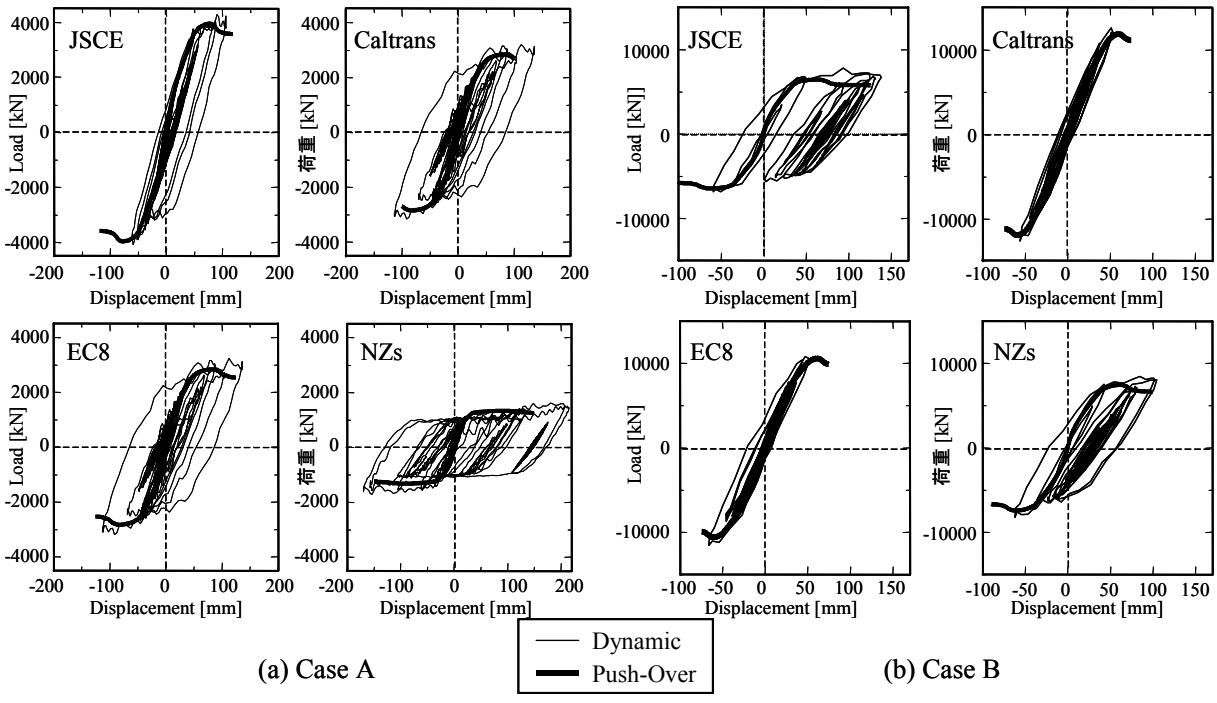

Figure 11 Analytical results (Dynamic)

6. Conclusions

In this study, four seismic design codes from different parts of the world were selected and applied to the design of two types of pier. Numerical analysis of this total of eight piers led to the following conclusions:

(1) Piers designed in accordance with the JSCE and NZs codes exhibited lower flexural capacity than those designed in accordance with Caltrans and EC8, but had sufficient shear capacity.
(2) Piers designed in accordance with Caltrans and EC8 exhibited higher flexural capacity than those designed in accordance with the JSCE and NZs codes. Though the EC8 pier in Case B showed a slightly lower shear margin, this was due to the method of selecting cross-sectional dimensions for the trial design. In an actual design procedure, piers designed according to the EC8 code would have a sufficient safety against shear failure.
(3) Trial design and numerical analysis of the piers revealed that the JSCE and NZs codes offer economical design approaches that ensure adequate safety against shear failure by relying on the plastic deformability of the member. On the other hand, Caltrans and EC8 are conservative design approaches that rely on the load-carrying capacity of the member.
(4) Since there are an unlimited number of solutions that meet the requirements of each code, the results obtained do not represent general solutions using the four seismic design codes. However, this comparison of the codes does reveal their notable characteristics.
(5) The lattice equivalent continuum model (LECM) was applied to the nonlinear dynamic analysis of reinforced concrete structures in this study. This model gives results that are similar to those obtained with other models, as shown in Fig. 13, with no appreciable defects arising during calculation [2]. LECMs are therefore considered applicable to the nonlinear dynamic analysis of reinforced concrete structures.

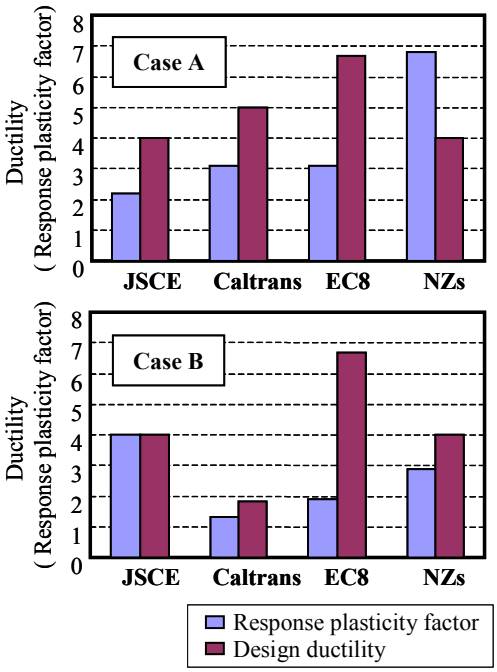

Figure.12 Response plasticity factor of pier

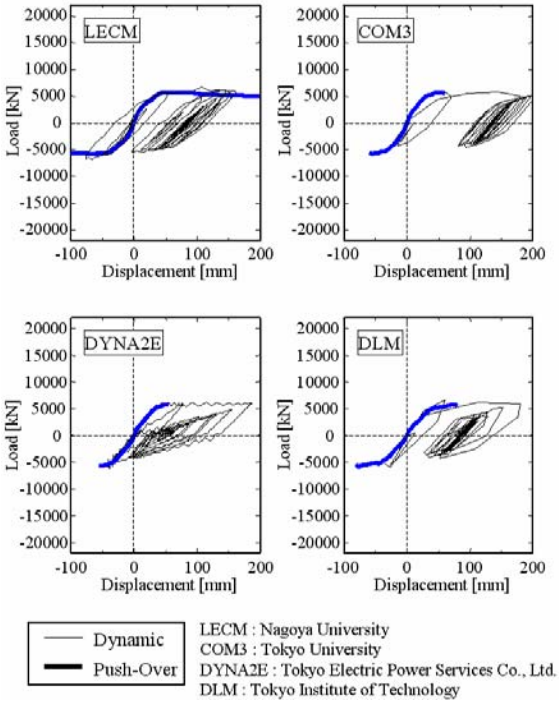

Figure 13 Comparison of analytical models

Acknowledgments

The authors express their sincere gratitude to Prof. Junichiro Niwa at Tokyo Institute of Technology, Mr. Sadaaki Nakamura of PC Bridge Co., Ltd., and Mr. Atsushi Mori of Japan Engineering Consultants Co., Ltd. for their advice regarding international design codes, as well as to Mr. Gouxing Yu of Oriental Construction Co., Ltd. and Assoc. Prof. Yasuaki Ishikawa of Meijo University for their advice regarding numerical analysis.

Appendix

The flowcharts for seismic design by the four design codes are given in Figures A1 to A4. And The bar arrangements in piers designed by the four design codes are shown in Figures A5 to 8A.

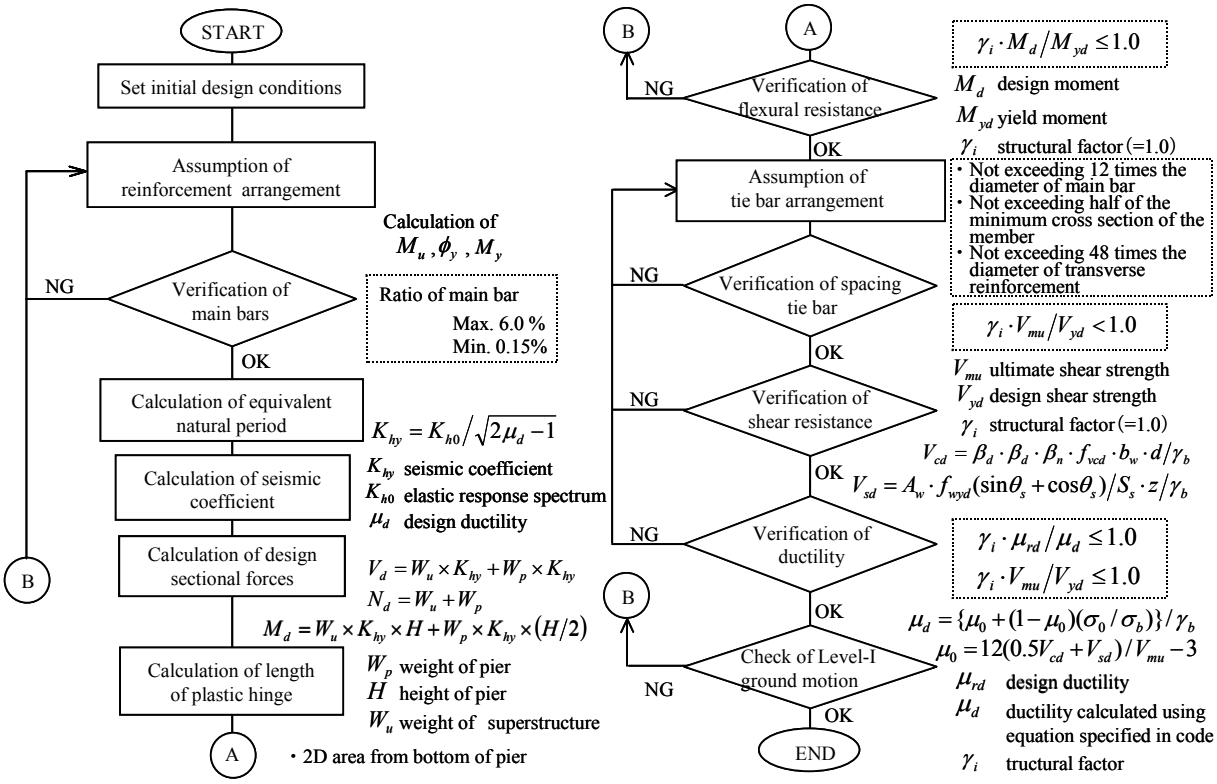

Figure A1 Flowchart of seismic design by JSCE

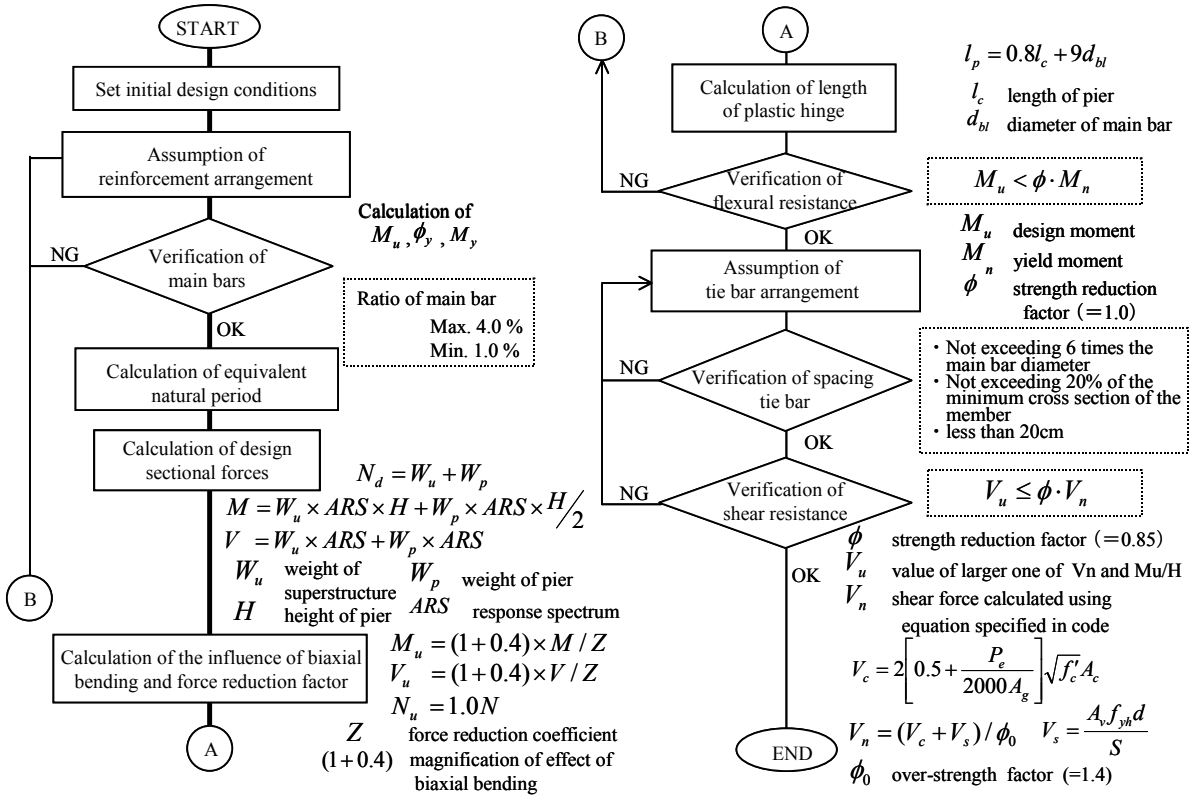

Figure A2 Flowchart of seismic design by Caltrans

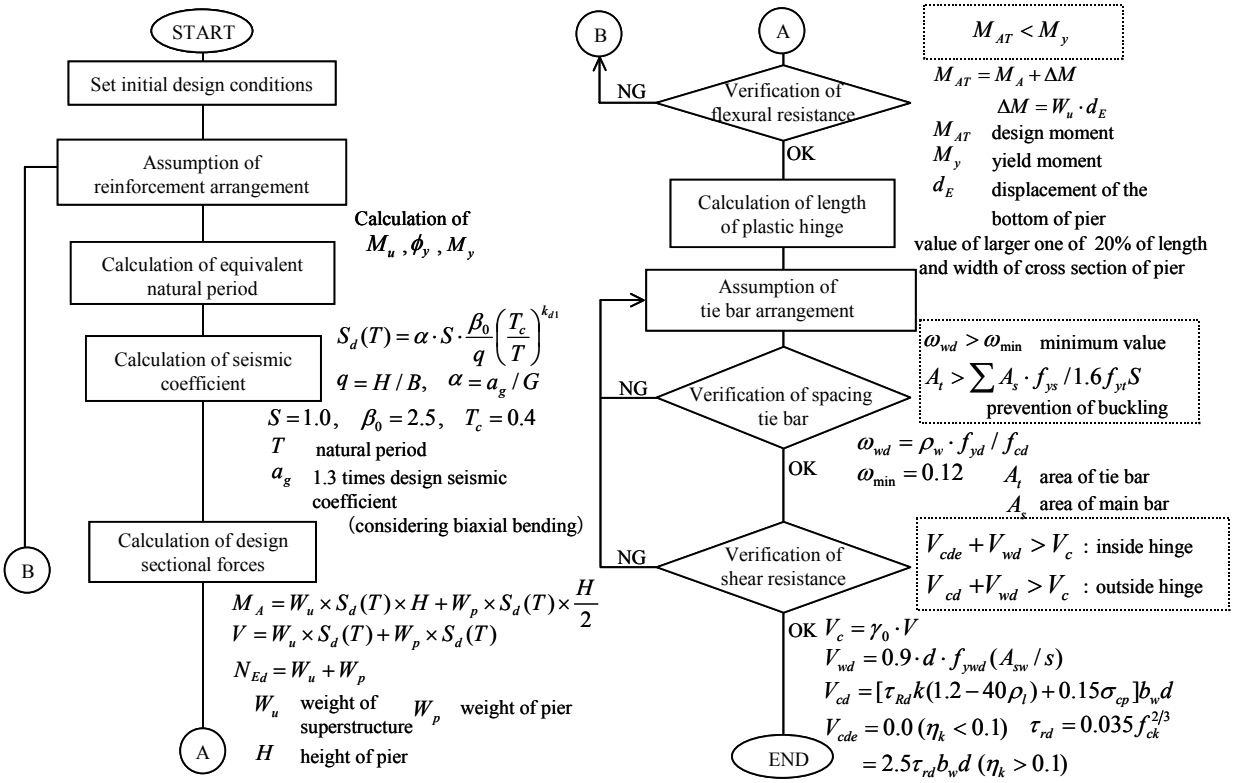

Figure A3 Flowchart of seismic design by EC8

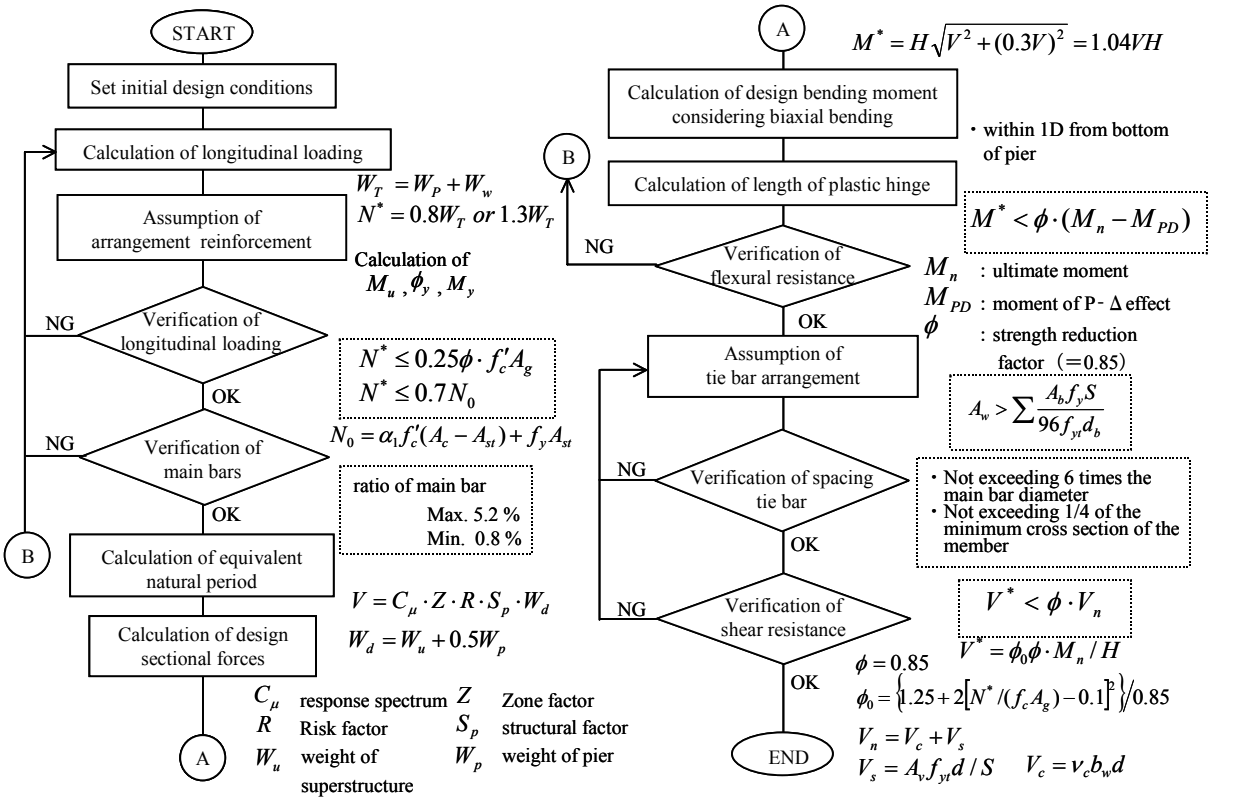

Figure A4 Flowchart of seismic design by NZs

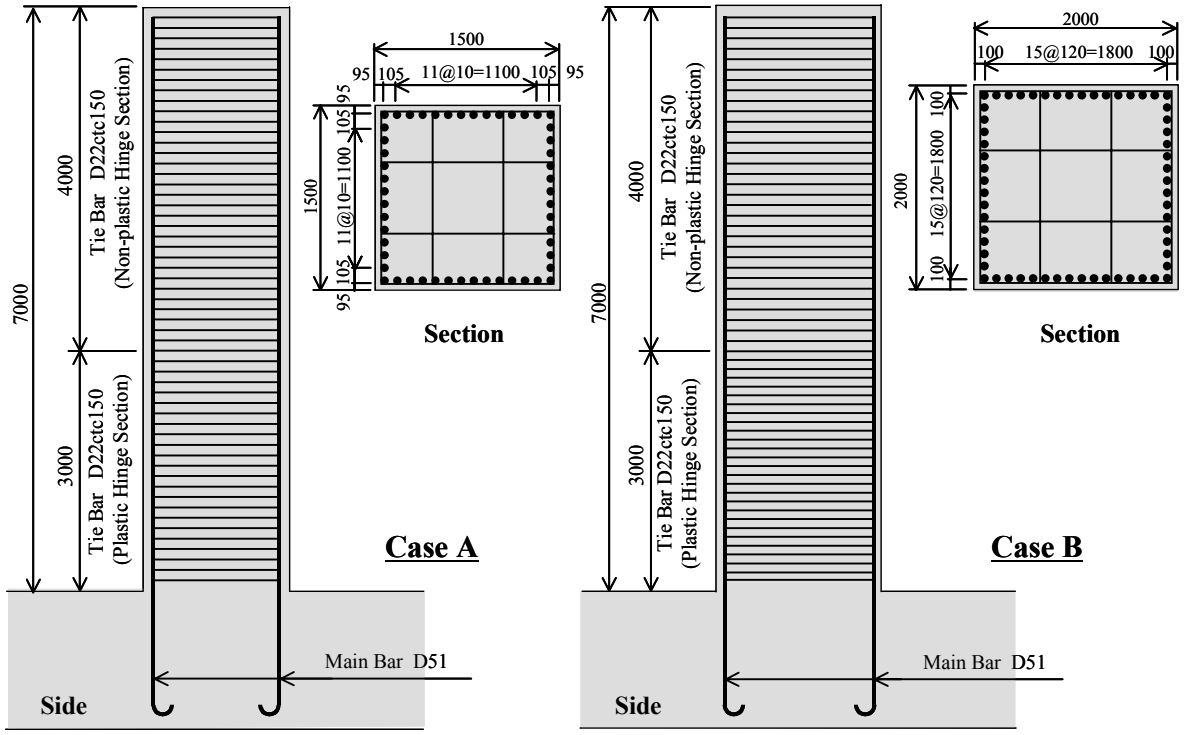

Figure A5 Arrangement of Reinforcement as Designed by JSCE

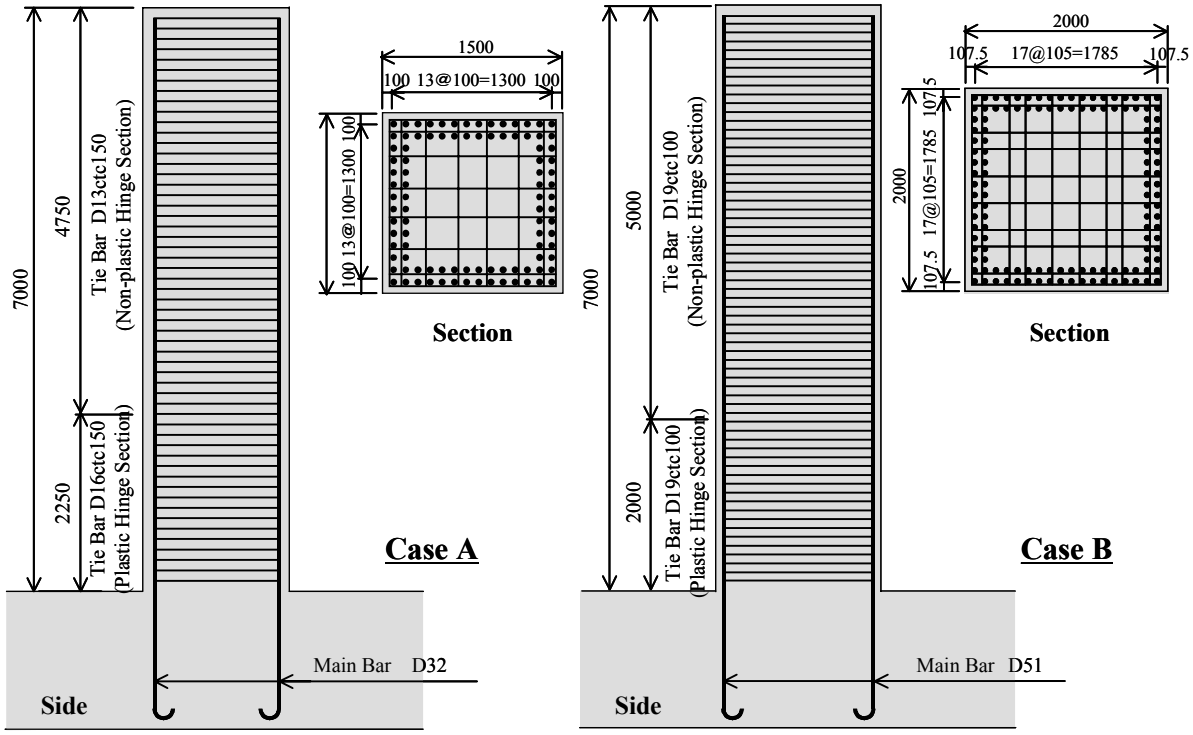

Figure A6 Arrangement of Reinforcement as Designed by Caltrans

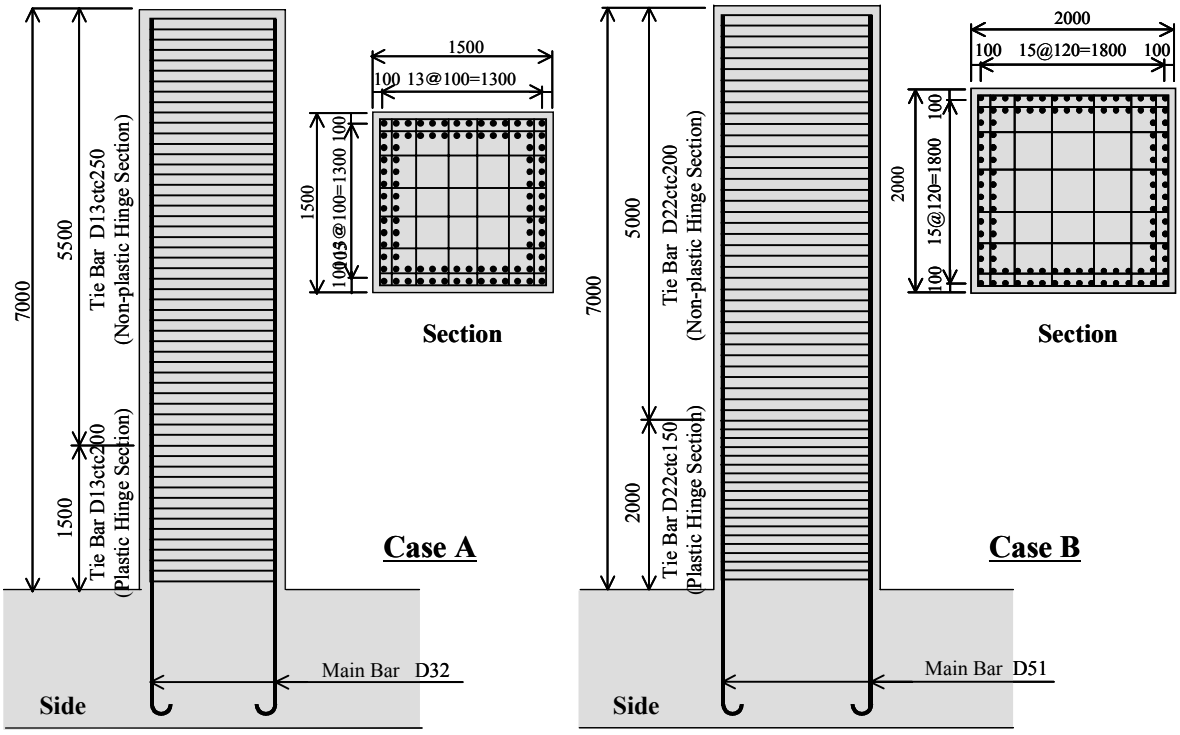

Figure A7 Arrangement of Reinforcement as Designed by EC8

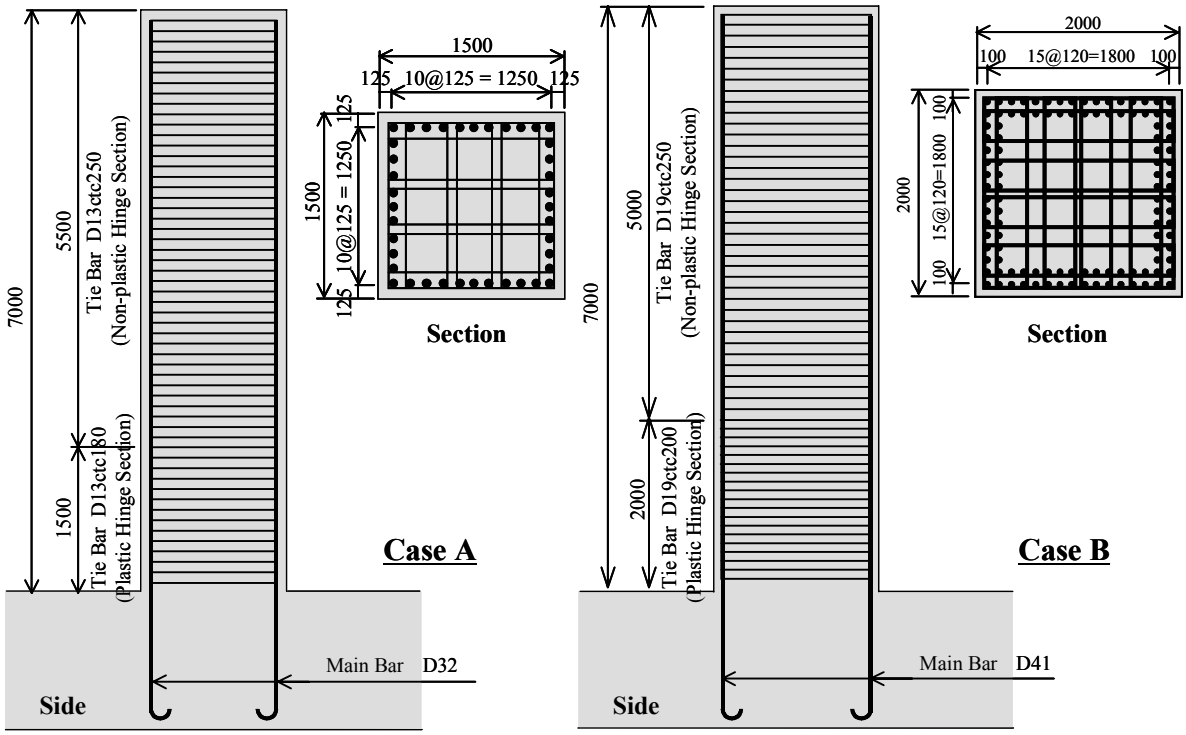

Figure A8 Arrangement of Reinforcement as Designed by NZs

References

[1] Tanabe, T.: Comparative Performance of Seismic Design Codes for Concrete Structures, Vol.1, Elsevier, 1999

[2] Tanabe, T.: Comparative Performance of Seismic Design Codes for Concrete Structures, Vol.2, Elsevier, 2000

[3] Kimata, H., Kongkeo, P., Ishikawa, Y., and Tanabe, T.: Nonlinear Dynamic Analysis of RC Piers designed by Four Major Seismic Design Codes, Proceedings of the Japan Concrete Institute, Vol.22, No.3, pp.1381-1386, 2000

[4] Kume, A., Yu, G., and Tanabe, T.: Analysis of RC Beam under Cyclic Loading Using Constitutive Law by the Equivalent Continual of Plane Lattices, Proceedings of the Japan Concrete Institute Vol.21, No.3, pp.103-108, 1999

[5] Tanabe, T., and Ahmad, S. I.: Development of Lattice Equivalent Continuum Model for Analysis of Cyclic Behavior of Reinforced Concrete, Proceedings of the Seminar on Post-Peak Behavior of RC Structures Subjected to Seismic Loads, Vol.2, pp.105-124, 1999

[6] Japan Society of Civil Engineering: Design Codes of Concrete Structures, Seismic Design Chapter, 1996

[7] Railway Technical Research Institute: Design Codes for Railway Structures, Seismic Design Chapter, 1999

[8] Japan Road Association: Specifications for Highway Bridges Part V [Seismic Design], 1996

[9] Ito, A., Niwa, J., and Tanabe, T.: Evaluation of Ultimate Deformation of RC Columns Subjected to Cyclic Loading Based on the Lattice Model, Journal of Materials, Concrete Structures and Pavements, JSCE, No.641/V-46, pp.253-262, 2000.2

[10] EL-Behairy, F. M., NIWA, J., and Tanabe, T.: Analysis of RC Columns under Pure Torsion using the Modified Lattice Model in Three Dimensions, Journal of Materials, Concrete Structures and Pavements, JSCE, No.634/V-45, pp.337-348, 1999.11

[11] Kollar, L., and Hegedus, I.: Analysis and Design of Space Frames by the Continuum Method, Elsevier, 1985

[12] Sonoda, K.: Structural Mechanics I, Asakura-shoten, pp.108-138, 1985

[13] Shibata, A.: Analysis of Seismic Structures, Morikita-shuppan, pp.97-112, 1981

[14] Tanabe, T., Higai, T., Umehara, H., and Niwa, J.: Concrete Structures, Asakura-shoten, 1992

[15] Mutsuyoshi, H: Tend of Seismic Design for Concrete Structures — Bridge Structures, Concrete Journal Vol.35, No.9, pp.3-11, 1997.9